

# The Response of Sea Levels to Typhoons in the Japan Sea

## Part I. The Response on the North Japanese Coast

Chol-Hoon HONG and Jong-Hwan YOON\*

*Research Center for Ocean Industrial Development, National Fisheries University of Pusan,  
Pusan 608-737, Korea*

*\*Research Institute for Applied Mechanics, Kyushu University, Fukuoka, Japan*

The response of sea levels to a typhoon in the north Japanese coast in the Japan Sea is investigated by using hourly sea level data(1966~1986) and a numerical shallow water model with high resolution(5'×5'). The observed sea level analysis shows (1) progressive waves exist between Simonoseki(SS) and Maizuru(MZ) with the mean phase speed of about 4 m/s during the passage of the typhoon, (2) the phase speed between Sasebo(SB) and HK(Hakata) is slower(about 1.7 m/s), and (3) the maximum sea level at HK is achieved about 0.5 day later than that of SS. In many aspects, the numerical model results correspond well to the above observed features. In the model the progressive waves are identified as a topographic wave with the phase speed of about 4 m/s. Before the typhoon passes through the Korea Strait/ the Tsushima Strait, the wave propagations along the Japanese coast are significantly influenced by the southwestward coastal jet induced by the wind stress parallel to the coast. The waves start to propagate northeastward along the coast when the coastal jet is weakened.

### Introduction

In summer and fall, many typhoons often pass through the Japan Sea, and give great influences on the circulation in the Japan Sea, especially in coastal area.

Isozaki(1968) reported that during the passage of typhoons, waves are generated along the north Japanese coast and propagate along the coast. He also showed that the responses of the sea level to the typhoon are very different in each typhoon. However, he could not show a detailed structure of sea level variation. Isoda *et al.*(1992a) suggested the existence of a topographic wave off San'in coast which may be related to the passage of typhoons, and Isoda(1993) explained the waves as mainly higher mode shelf waves based on an analytical and linear shallow numerical model forced by an ideal wind.

The object of this study is to investigate the wave propagation characteristics along the north Japanese coast for the 'strait-passing typhoon', which enter the Japan Sea after passing the Korea Strait/the Tsushima Strait(Fig. 1) from the East China Sea, by using the sea level analysis and the numerical shallow water model.

### Waves along the north Japanese coast in observations

In the present study 'strait-passing typhoons' (TP7911, TP8410, TP8520, and TP8616) are adopted to investigate the detailed structure of the sea level variation along the north Japanese coast. Here the symbol, e.g., TP8410 indicates the 10th typhoon in 1984. The hourly sea level data from 1966 to 1986 obtained by the Japan Meteorological Agency

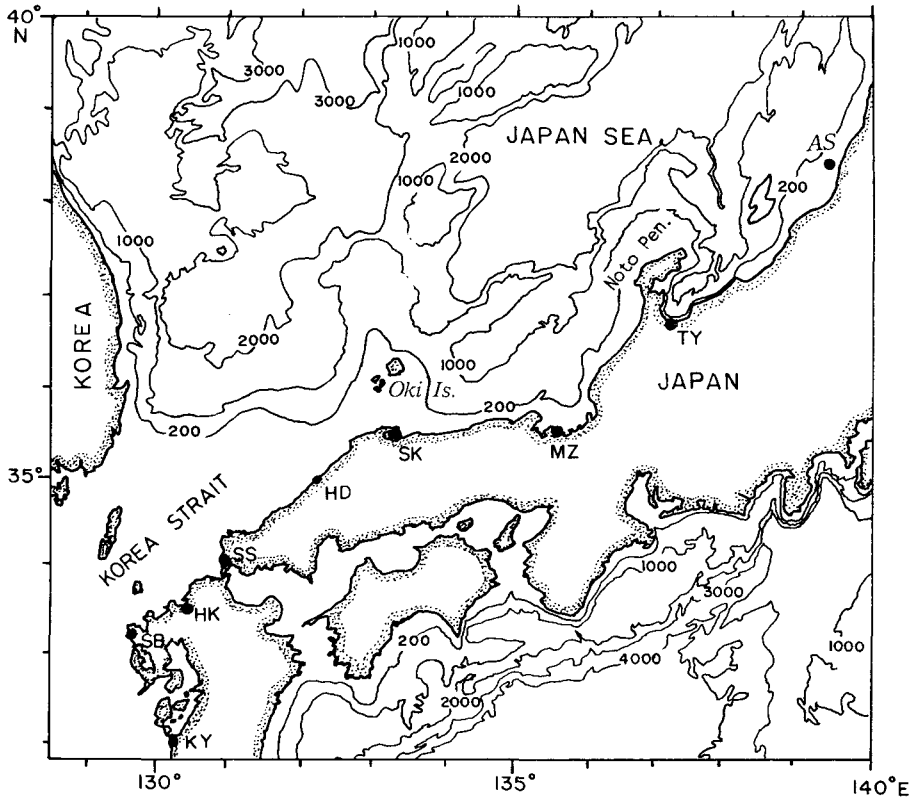


Fig. 1. The topography around the Korea Strait. Depths are in meters. The tidal stations are shown.

(JMA) and Marine Safety Agency(MSA) in Japan were analyzed. The tidal stations are shown in Fig. 1, and their locations are listed in Table 1. The tracks of the four typhoons are shown in Fig. 2, with each typhoon's attribute in the passing periods through the Korea Strait listed in Table 2.

Fig. 3 shows the time series of sea level variations for these four typhoons. The passing periods through the Korea Strait are adjusted to be same among these typhoons along the axis of time, and are indicated by two vertical solid bars with the 12 hour interval. Cross marks indicate the peak sea levels at each station. The time series show the anomalies of the sea levels from mean sea levels, and the tidal components in sea levels were removed by the low-pass filter(Miyata, 1970). The time series for TP8410 at HK do not show a complete form, due to the lack of data caused by the severe storm. The sea level variation east of TY(Toyama) is analyzed by using the sea level data of AS(Awasima island) in the shallow coastal area(about 15 km off the coast). In the early stage the sea level

Table 1. List of the tidal stations from MSA (Marine Safety Agency) and JMA(Japan Meteorological Agency)

Station	Location	Authority
Sasebo(SB)	33°09'N 129°43'E	MSA
Hakata(HK)	33°33'N 130°24'E	MSA
Simonoseki(SS)	33°58'N 130°57'E	JMA
Hamada(HD)	34°54'N 132°04'E	JMA
Sakai(SK)	35°33'N 133°15'E	JMA
Maizuru(MZ)	35°28'N 135°23'E	MSA
Toyama(TY)	36°46'N 137°13'E	JMA
Awasima(AS)	38°28'N 139°14'E	MSA

Table 2. Attributes of typhoons in the passing time through the central part in the Korea Strait

Typhoon	Date	Central p. (mb)	Direction	Speed (km/h)
TP7911	1979. 8.26 21 : 00	994	ENE	25~40
TP8410	84. 8.21 15 : 00	970	NE	25~35
TP8520	85.10. 5 15 : 00	990	ENE	35~40
TP8616	86. 9.21 09 : 00	1000	NE	70

at each station is low, but as the typhoon approaches the Korea Strait, the sea level starts to increase rapidly. The maximum sea levels at SB and SS in the Korea Strait, and TY and AS east of Noto Peninsula are achieved as each typhoon passes over each station, while those between HD and MZ, are achieved in about 0.5 to 2 days after the typhoon has passed. It should be noted that the maximum sea level at HK is seen about 0.5 day later, than that of SS, i.e., the maximum at HK is achieved several hours after the passage of the typhoon. Tracking of the maximum sea levels indicates the existence of a progressive wave between SS and MZ. The mean progressive speed is estimated to be 3.5 to 4 m/s. However, it seems to be difficult to identify the progressive wave between HK and SS. It is noted that the phase speed between SB and HK is about 1.7 m/s which is slower than that between SS and MZ. The time series also show

two peaks at TY: one of the peaks is seen during the passage of the typhoon, and the other appears at one to three days after passing of the typhoon, although the one for TP8410 is not clear. In the east of Noto Peninsula the propagation of disturbance is obscure. It seems most probable that it is difficult for a disturbance to directly propagate from MZ to east of Noto Peninsula due to the bottom topographic structure around the Peninsula.

Form these results it is concluded that according to the way of reponse of sea levels to a typhoon, the area may be divided roughly into three parts, i.e. the entrance of the Korea Strait(between SB



Fig. 2. Rough paths of four typhoons, TP7911, TP8410, TP8520 and TP8616 which passed through the Korea Strait. The solid circles on the tracks indicate the positions of center of the typhoons at 0900 local time every day.

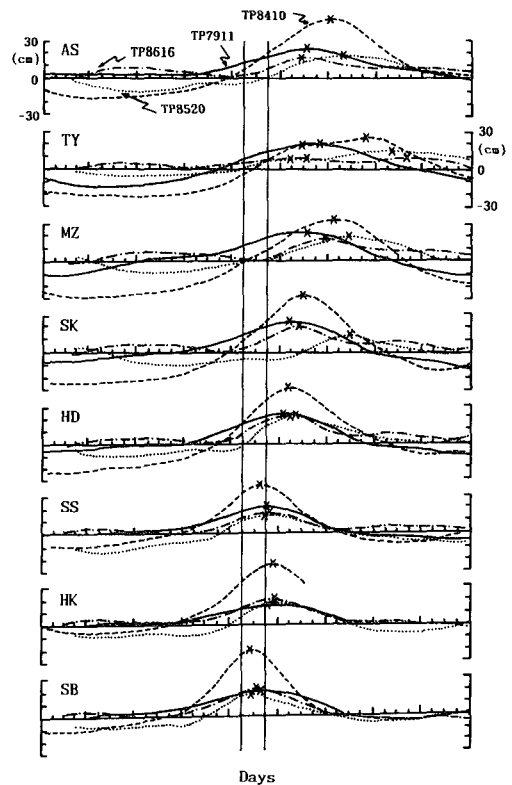


Fig. 3. The time series of demeaned sea level variations for four typhoons, TP7911(solid line), TP8410(broken line), TP8520(dotted line) and TP8616(dot-dashed line). The periods of passing through the Korea Strait are adjusted to be the same in these typhoons along the axis of time. The two vertical solid bars for 12 hours intervals indicate the periods of passing through the Korea Strait for the typhoons. The cross marks indicate the peaks of sea levels.

and SS), east of Noto Peninsula, and the area between SS and MZ.

The results are summarized as follows:

(1) According to the way of the response of the sea levels to a typhoon the area can be divided roughly into three parts, i.e. the entrance of the Korea Strait(between SB and SS), east of Noto Peninsula, and the area between SS and MZ.

(2) Progressive waves exist between SS and MZ with the mean phase speed of about 4 m/s in the passing period of 'strait-passing typhoon'.

(3) The phase speed between SB and HK is slow(about 1.7 m/s).

(4) East of Noto peninsula, the wave propagation is obscure.

In the following chapters we will investigate the mechanism for the sea level variations in the numerical shallow water experiment.

### Model

The experiment is conducted on a spherical coordinate system with 5'×5' horizontal resolution, by using the following shallow water equations:

$$\begin{aligned} \frac{\partial}{\partial t} U + \frac{1}{\cos\phi} \frac{\partial}{\partial \lambda} (uU) + \frac{1}{\cos\phi} \frac{\partial}{\partial \phi} (uV\cos\phi) \\ - \frac{uV}{a} \tan\phi - fV = \\ - \frac{gH}{\cos\phi} \frac{\partial}{\partial \lambda} (\eta - \eta_0) + \frac{\tau^\lambda}{\rho} - F^\lambda + T^\lambda, \end{aligned} \quad (1)$$

$$\begin{aligned} \frac{\partial}{\partial t} V + \frac{1}{\cos\phi} \frac{\partial}{\partial \lambda} (vU) + \frac{1}{\cos\phi} \frac{\partial}{\partial \phi} (vV\cos\phi) \\ + \frac{uV}{a} \tan\phi + fU = \\ - \frac{gH}{a} \frac{\partial}{\partial \phi} (\eta - \eta_0) + \frac{\tau^\phi}{\rho} - F^\phi + T^\phi, \end{aligned} \quad (2)$$

$$\frac{\partial}{\partial t} \eta + \frac{1}{\cos\phi} \frac{\partial}{\partial \lambda} U + \frac{1}{\cos\phi} \frac{\partial}{\partial \phi} (V\cos\phi) = 0. \quad (3)$$

The notations are conventional:  $\phi$  is latitude,  $\lambda$  the longitude,  $\eta$  the sea surface elevation,  $a$  is the earth's radius,  $H=h+\eta$  the water depth,  $h$  the depth from mean sea level to bottom,  $\rho$  density of water,  $\eta_0$  isostatic elevation. The  $(\tau^\lambda, \tau^\phi)$  are  $(\lambda, \phi)$  components of wind stress, and the  $(U, V)(\lambda, \phi)$  components of the volume transport, i.e.

$$U = \int_{\eta}^{\eta_0} u dz, \quad V = \int_{\eta}^{\eta_0} v dz. \quad (4)$$

The  $(F^\lambda, F^\phi)$  are  $(\lambda, \phi)$  components of bottom friction, given as

$$(F^\lambda, F^\phi) = \gamma(u, v) \sqrt{u^2 + v^2}, \quad (5)$$

where  $\gamma = 2.3 \times 10^{-4}$  is the resistance coefficient. The  $(T_\lambda, T_\phi)$  are  $(\lambda, \phi)$  components of horizontal viscosity, given as

$$T_\lambda = A_h H \left( \Delta u - \frac{1}{a^2 \cos^2 \phi} u - \frac{2}{a^2 \cos^2 \phi} \frac{\partial}{\partial \lambda} (v \sin \phi) \right), \quad (6)$$

$$T_\phi = A_h H \left( \Delta v - \frac{1}{a^2 \cos^2 \phi} v + \frac{2 \sin \phi}{a^2 \cos^2 \phi} \frac{\partial u}{\partial \lambda} \right), \quad (7)$$

where  $A_h = 10^{-7} \text{ cm}^2 \text{ s}^{-1}$  is horizontal eddy viscosity coefficient, and the operator  $\Delta$  is

$$\Delta = \frac{1}{a^2 \cos^2 \phi} \frac{\partial^2}{\partial \lambda^2} + \frac{1}{a^2 \cos \phi} \frac{\partial}{\partial \phi} \left( \cos \phi \frac{\partial}{\partial \phi} \right). \quad (8)$$

The data of bottom topography are obtained from JODC(Japan Oceanographical Data Center). The depth deeper than 3600 m is set to be 3600 m in the model. The model ocean includes the East China Sea, the Yellow Sea, and the Japan Sea, which has the range of  $31^\circ \times 25^\circ$  in the direction of north-south and east-west, respectively. The topography around the Korea Strait in the model and the tidal stations are shown in Fig. 4

The initial condition is given by

$$(u, v) = \eta = 0 \text{ at } t = 0$$

and the boundary condition for velocity is assumed as  $(u, v) = 0$ , where  $(u, v)$  are velocity components in the zonal and meridional direction, respectively. The flow field is analyzed by the stream function obtained from rotational components of velocity.

The air pressures and winds in the model typhoon are given by Fujita's formula(1952) and Miyazaki *et al.*(1961), respectively. The typhoon(TP 8410) is adopted as a model typhoon of the 'strait-passing typhoon'. The detailed track is shown in Fig. 5(see Hong and Yoon(1992) for detailed description of the model).

### Result

Fig. 6 shows the time series of sea level variations at each station for TP8410 obtained by the observation(solid line) and the model(dotted line). To compare the result with the observation, the ti-

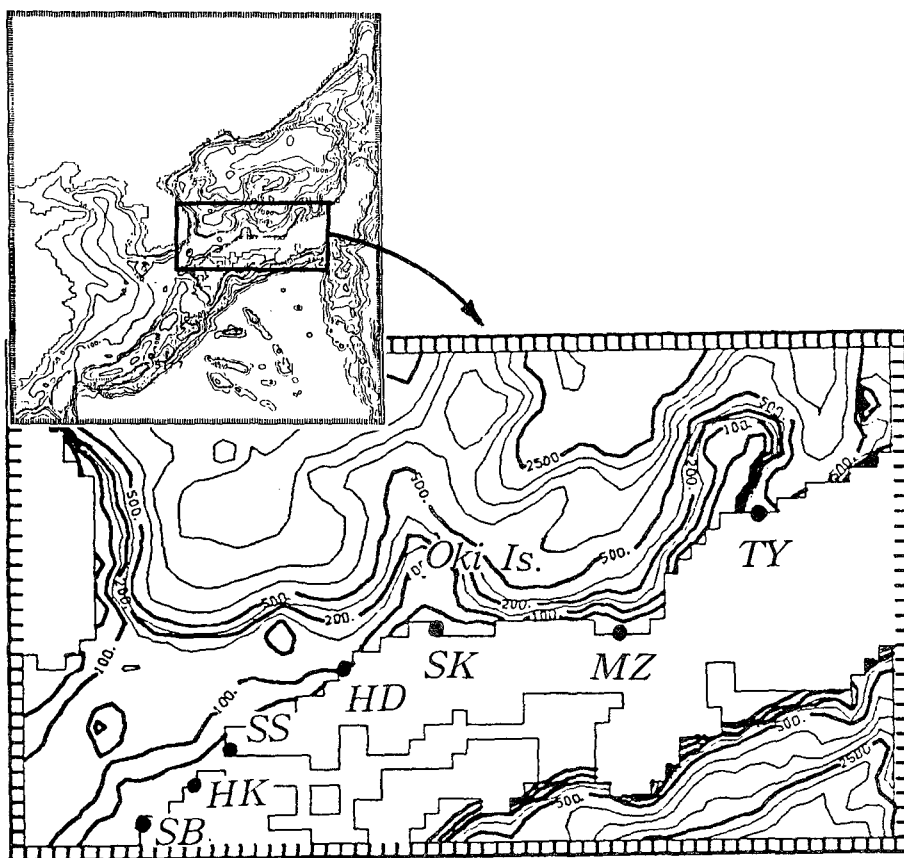


Fig. 4. The topography around the Korea Strait in the model and also tidal stations. The drastic topographical change in continental slope is noted.

dal components were filtered out from the time series of the model by the low-pass filter (Miyata, 1970). In many aspects, the results in the model correspond well to the observations, that is:

- (1) The waves in the model propagate from SS to SK with about 4 *m/s* of phase speed.
- (2) The phase speed between SB and HK is about 1.7 *m/s*.
- (3) The maximum sea level at the stations west of SK except for SS are obtained almost same as observation.

Differences between the observation and the model are as follows:

- (1) In the model, the time-lag (about 3 or 5 hours in the observation) among the maximum sea levels in the achieving time at HK and SS is not seen, i.e. the achieved times for the maximum sea levels

at two stations are identical.

- (2) From the maximum sea levels east of SK, it can be concluded that the property of progressive wave disappears in this region.
- (3) The values of maximum sea levels in the model tend to be higher than that of the observations by 5 to 10 *cm*.

Next, we investigate the sea level changes in horizontal variations of surface elevations and velocity field.

Fig. 7 shows the horizontal variations of surface elevations (upper) and velocity fields (lower) at 12:00 local time, August 19, 1984 (hereafter referred to as 191200) (Fig. 7a) and 201200 (Fig. 7b). The surface elevation in the Japanese coast shows negative values and corresponds well to the time series shown in Fig. 6. In the velocity field, the south-

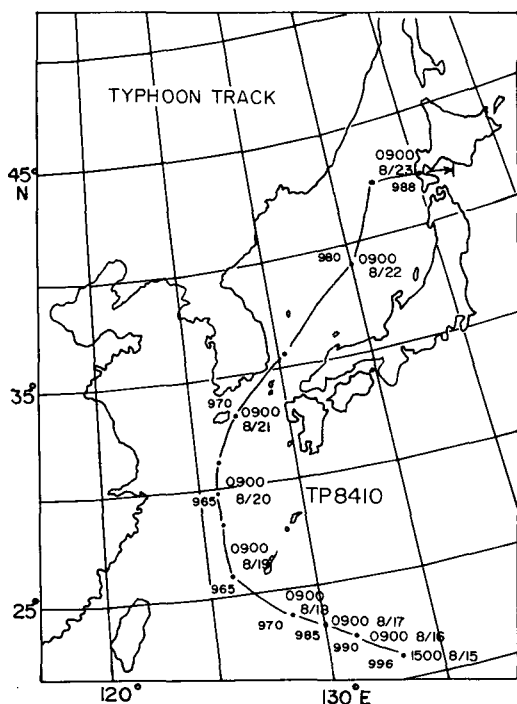


Fig. 5. The tracks of TP8410(August, 1984) used in the model. The numerals assigned to the points on the track indicate the central pressure, day, and time.

westward coastal jet along the Japanese coast west of MZ is formed due to the wind stress parallel to the coast(Hong and Yoon, 1992). In these periods the surface elevation in the north Japanese coast is determined by the isostatic rise due to atmospheric pressure and the water pressure with balancing to the geostrophic flow. Although the typhoon approaches the Korea Strait, the surface elevation in the Japanese coast are still low due to the coastal jet as shown in Fig. 7b.

The surface elevations and velocity field at 202100 and 210900 are shown in Fig. 8. The southwestward coastal jet becomes stronger along the Japanese coast and the high sea levels around the Korean coast already propagate northward along the east Korean coast. The propagation of the high sea level along the Japanese coast might be decelerated due to the southward coastal jet. This might be the reason why the phase speed between SB and HK is slow (about 1.7 m/s).

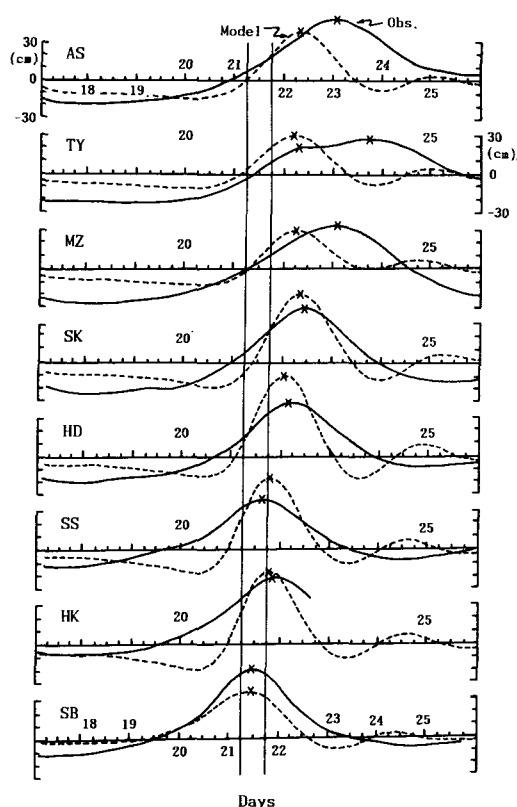


Fig. 6. The time series of sea level variations at each station for TP8410 in the model(dotted line) and the observation(solid line).

Figure 9 shows the surface elevation(upper), velocity field(middle) and stream function(lower) at 211500(Fig. 9a) and 220000(Fig. 9b). In the surface elevation and velocity field in Fig. 9a, so called 'stationary state' of high sea level is destroyed by the northeastward strong current in the Japanese coast in the Korea Strait. This is caused by the southwest wind accompanied by the typhoon through the Korea Strait, and permits the high sea level propagation along the Japanese coast(upper maps in Fig. 9a,b). On the other hand, it is noticed that in the stream function field, a cyclone accompanied by the typhoon is formed in the southeast sea of Korea as shown in Fig. 9b(lower). We shall consider this point in the later part of this paper.

Fig. 10 shows the space-time diagram of the surface elevation along the north Japanese coast in

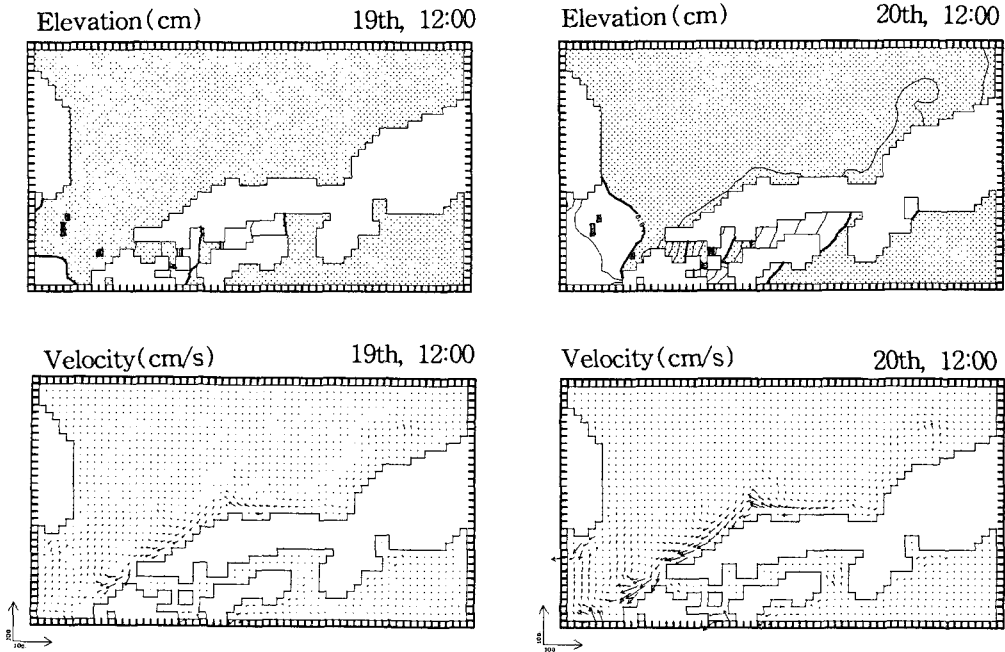


Fig. 7. The surface elevations(upper panel) and velocity fields(lower panel) at (a) 1200 local time, 19 August, 1984(hereafter 191200) and (b) 201200. Shade parts indicate negative field of the surface elevations.

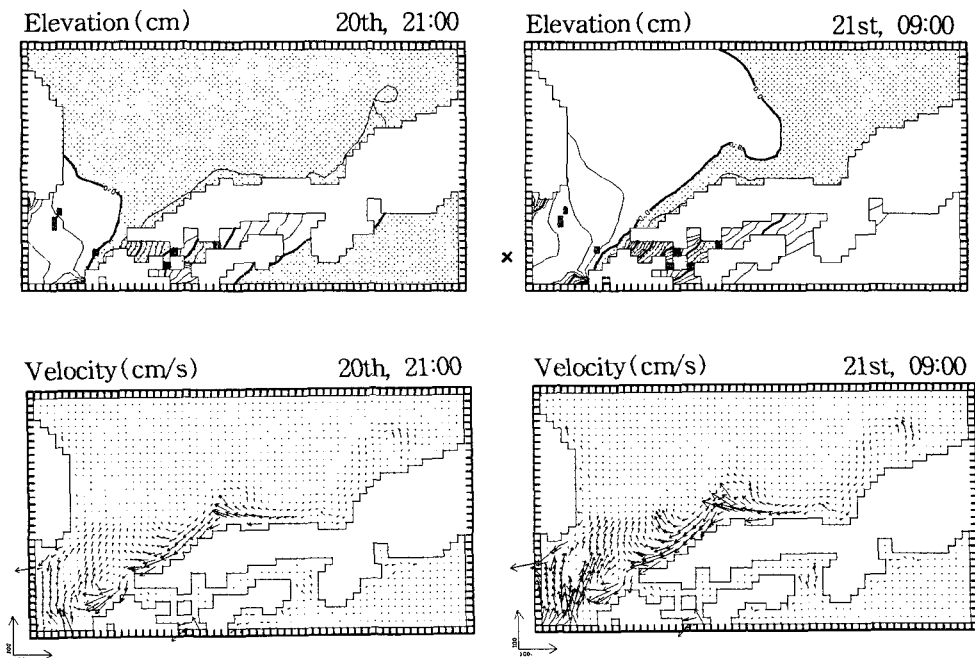


Fig. 8. As in Fig. 7 except for at (a) 202100 and (b) 210900.

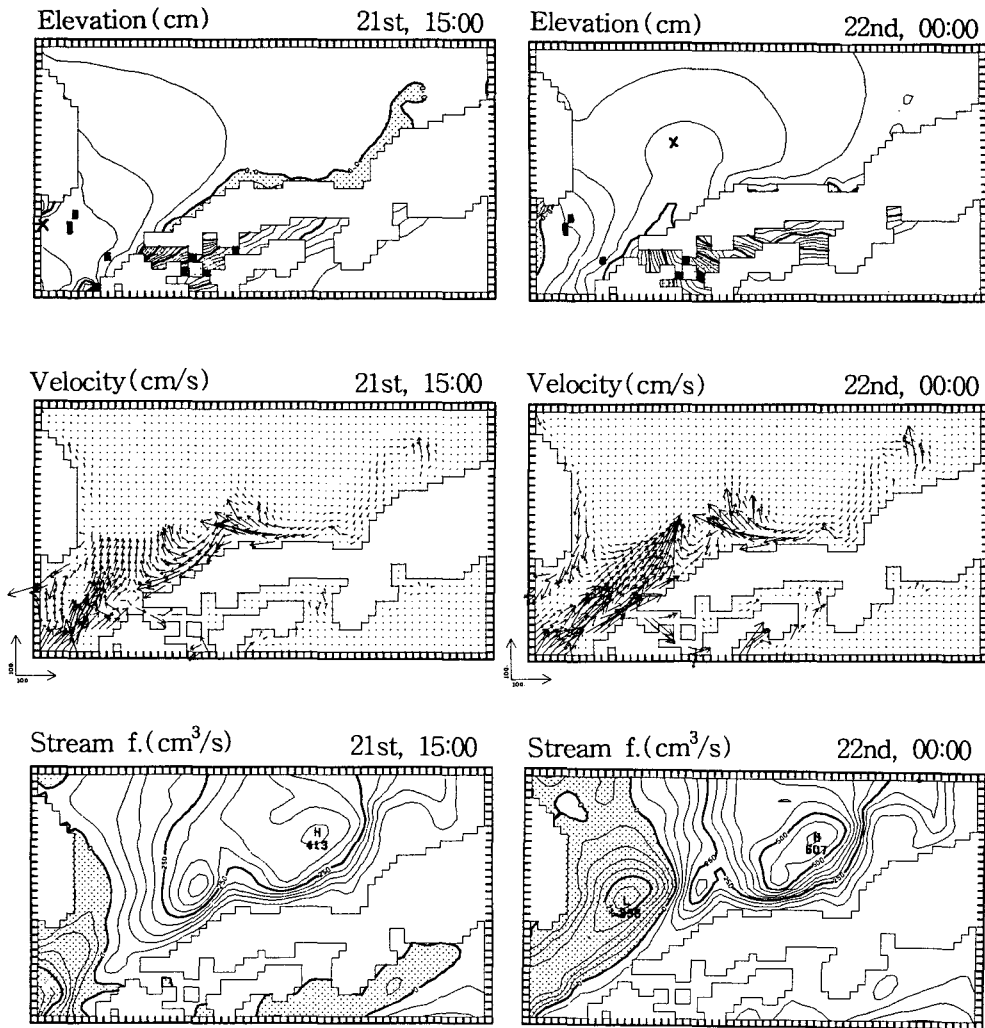


Fig. 9. The surface elevation(upper panel), velocity field(middle panel) and stream function(lower panel) with C.I.  $=10^{12}cm^3/s$  at (a) 211500 and (b) 220000.

Fig. 1. The width of two horizontal bars indicates the passing period(12 hours) of the typhoon through the Korea Strait. As we pointed out above, the 'stationary state' of the high sea level around SB is well identified in the propagation speed of the gradient of the contours before passing of the typhoon through the Korea Strait. The progressive speed of the high sea level is calculated to be about 4 m/s from the gradient of the thick solid line. This value corresponds well to the values(4.25 m/s) between SS and SK as shown in Fig. 6. However, the gradient of sea level east of SK is

shown almost the same phase in time. This shows that the wave along the Japanese coast does not propagate east of SK in the model. However, the stream function fields every 3 hours from 220300 to 221800 in Fig. 11 show that in the offshore region, the wave propagates eastward along the geostrophic contours with about 1.8 m/s. This suggests that Oki island can greatly influence eastward wave propagation along the Japanese coast between SK and MZ.

The oscillations of about 2.5 days period, which has been pointed out by Hong and Yoon(1992) as



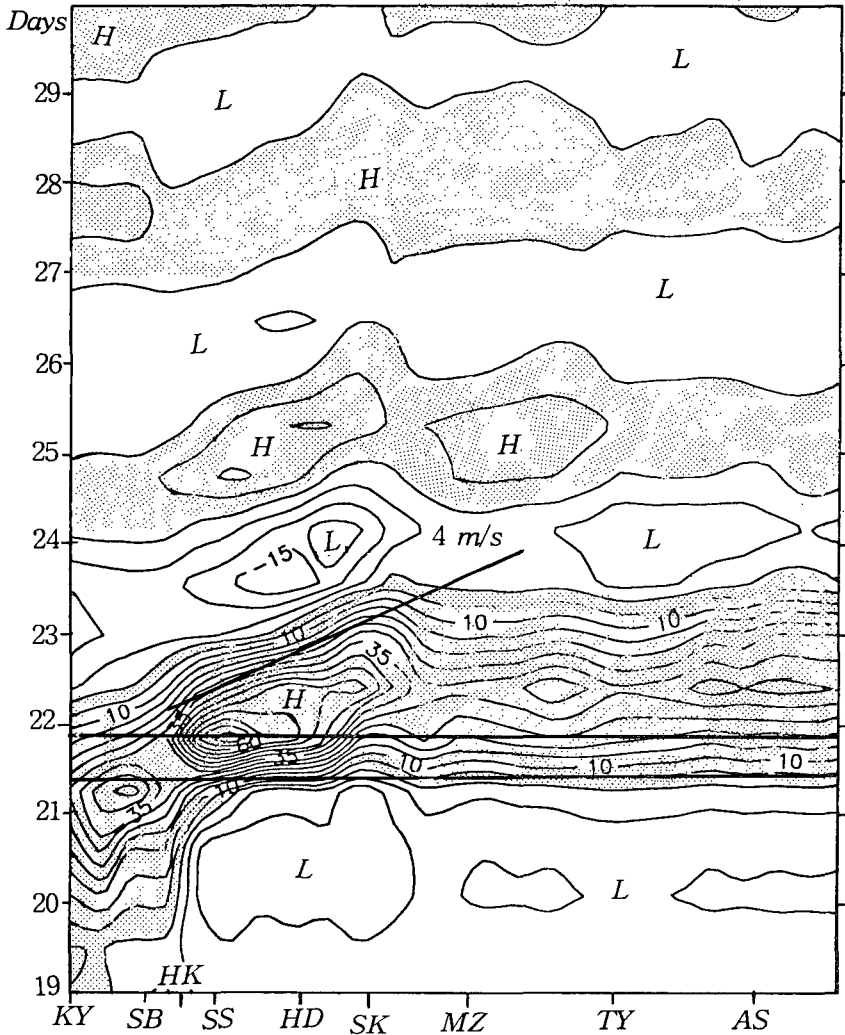


Fig. 10. The space-time diagram of surface elevation along the north Japanese coast in Fig. 1. Two horizontal lines indicate the period(12 hours) of the passing of the typhoon in the Korea Strait. The interval of contour is 5cm. The beginning point(KY) is the west coast of Kyushu in Japan.

a basin scale oscillation, are seen in Fig. 9. Fig. 12 shows the stream function fields every 6 hours from 222100 to 261500. This shows that the cyclone in the southeast sea of Korea formed by the typhoon, as indicated above, propagates along the continental shelf with a phase speed of about 2 to 3 m/s. Considering the speed and progressive direction of the cyclone, it indicates probable progression as a topographic wave.

### Conclusions and Discussions

The present study investigated the response of sea level along the Japanese coast to typhoons through the data analysis of sea level and the numerical experiment. The conclusions by the analysis of hourly sea level data for the strait-passing typhoon, between 1966 to 1986 are as follows:

- (1) According to the response characteristics of

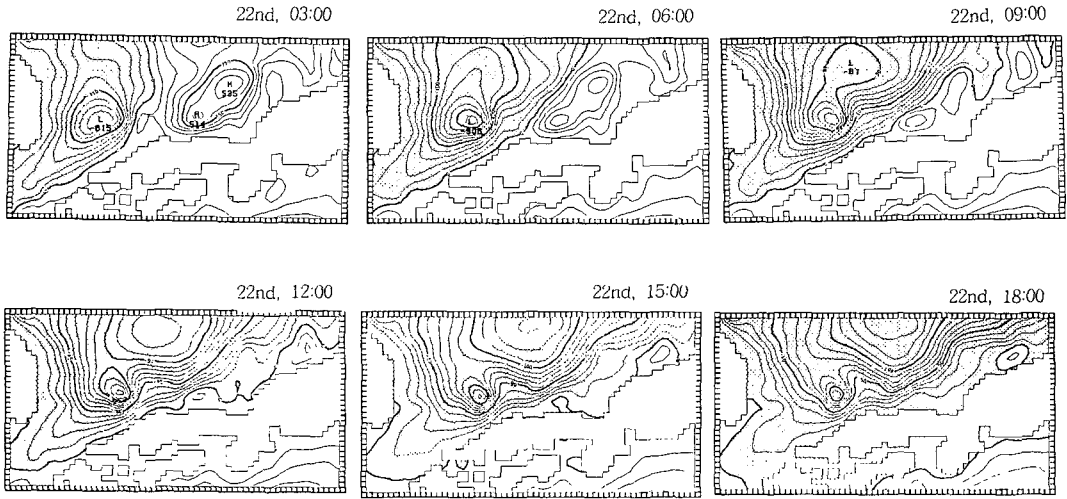


Fig. 11. The stream function fields every 3 hours from 200300 to 201800 with C.I.= $10^{12}cm^3/s$ .

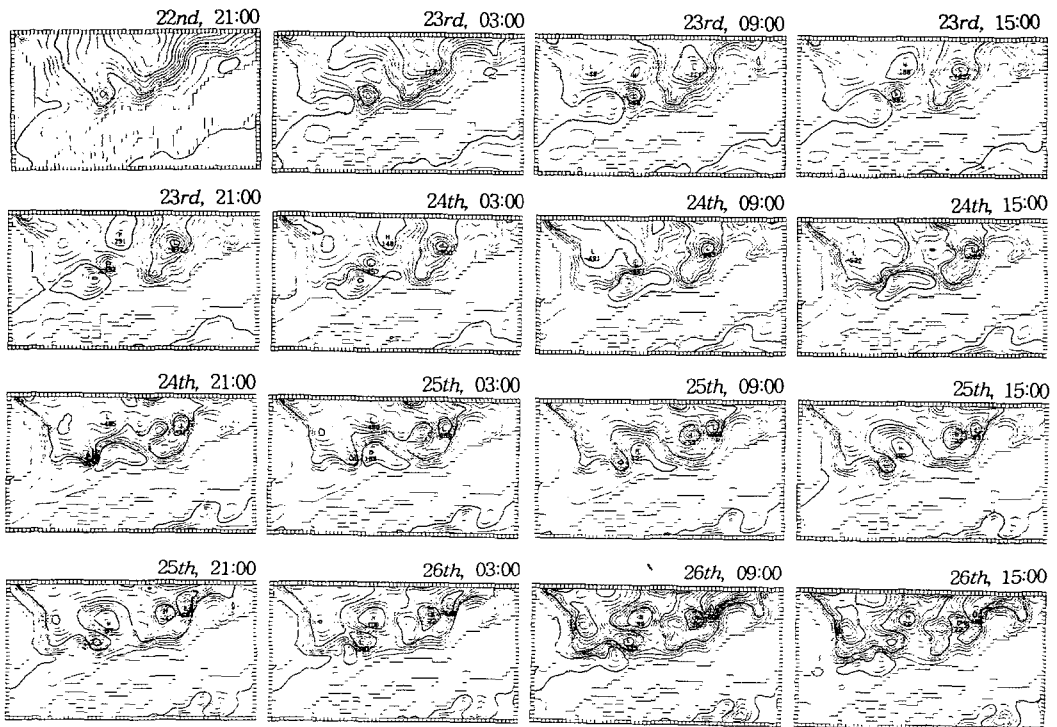


Fig. 12. Same as Fig. 11 except every 6 hours from 222100 to 261500 with C.I.= $10^{11}cm^3/s$ .

sea levels to typhoons the area can be divided roughly into three areas, i.e. the entrance of Korea Strait(between SB and SS), east of Noto Peninsula, and the area between SS and MZ.

(2) Progressive waves exist between SS and

MZ with the mean phase speed of about 4 m/s.

(3) The phase speed between SB and HK is slow(about 1.7 m/s).

(4) In the east of Noto Peninsula, the wave propagation is obscure.

In numerical shallow water model with  $5' \times 5'$  in horizontal resolution, the progressive 4 m/s of phase speed. Before the passage of the typhoon through the Korea Strait the wave propagation is significantly influenced by the southwestward coastal jet in the north Japanese coast due to the wind stress parallel to the coast. As the typhoon passes through the Korea Strait, the southwestward coastal jet becomes weak and the northeastward currents develop due to strong southwesterly winds and then the high sea level starts to propagate northeastward along the coast

Although the model is successful in reproducing the propagation of wave with a realistic phase speed west of SK, it is not successful east of SK.

The reason seems to be due to the resolution of the topography in the area. That is, if geostrophic contours are broken down on the continental shelf, topographic waves would not propagate further. Thus, it seems that the grid interval in the model with  $5' \times 5'$  might be insufficient to show an adequate resolution of the continental shelf east of SK as shown in Fig. 4. Due to the same reason, Yoon (1991) did not represent numerically a realistic velocity field east of Noto peninsula.

In the time of the maximum sea levels the model also did not reproduce the time lag (about 5 hours) in the observation (Fig. 6) between HK and SS. This may be related to the storm surge in the Seto Island Sea through the Strait of Kanmon, connecting the Korea Strait to the Seto Island Sea, as indicated by Isozaki (1968). The grid size in the model is not sufficient to show the resolution of the strait.

Recently, Isoda et al. (1992b) reported that the disturbance along sharp continental slope in the south east sea of Korea propagates eastward as a baroclinic topographic wave with 7 to 10 cm/s of phase speed, based on the analysis of temperature data measured by a submarine telephone cable on the shelf between Korea and Japan. Our model also shows that a barotropic topographic wave exists in this region, as shown in Fig. 10 and Fig. 12. This suggests that there will be topographic waves in another region with sharp topographic slope in the Japan Sea, e.g., Yamato Basin.

To investigate the response of sea level to typhoon on the east Korean coast in the Japan Sea will be our next subject.

## Acknowledgement

This research was supported by the Basic Science Institute Program of the Ministry of Education, Republic of Korea in 1991.

## References

- Fujita, T. 1952. Pressure distribution within typhoon. *Geophys. Mag.*, 23, 437~451.
- Gill, A. E. 1982. *Atmosphere-ocean dynamics*. Academic Press, New York. 99pp.
- Hong, C. H. and J. H. Yoon. 1992. The effect of typhoon on the coastal sea level variations in the Tsushima Straits (in Japanese). *J. Oceanogr. Soc. Japan (Umi no Kenkyu)*, 1(5), 225~249.
- Isoda, Y., T. Muratama and T. Tamai. 1992a. Variabilities of current and water temperature due to meteorological disturbances on the shelf off San'in coast (in Japanese). *Cont. Shelf Res.*, 11, 167~182.
- Isoda, Y. and H. Oomura. 1992b. Temporal and spatial variations in the Bottom Cold Water on the shelf off San'in coast, Japan. *La Mer* 30, 263~274.
- Isoda, Y. 1993. Generation mechanism of higher mode nondispersive shelf waves by wind forcing. *J. Oceanogr.* 49(5), 535~549.
- Isozaki, I. 1968. An investigation on the variations of sea level due to meteorological disturbances on the coast of Japanese islands (II) - Storm surges on the coast of the Japan Sea. *J. Oceanogr. Soc. Japan*, 24(4), 178~190.
- Miyata M. 1970. A study of the effect of local and distant weather on sea level in Hawaii. Ph.D. Thesis, University of Hawaii.
- Miyazaki, M., T. Ueno and S. Unoki. 1961. Theoretical investigation of typhoon surges along the Japanese coast. *Oceanogr. Mag.*, 13, 51~75.
- Yoon, J. H. 1991. The branching of the Tsushima

Chol-Hoon HONG and Jong-Hwan YOON

Current. Report of RIAM, Kyushu University,  
38(108), 1~21.

---

Received October 4, 1993

Accepted November 6, 1993

## 동해연안역 해수면변동에 미치는 태풍의 영향

### I. 일본 북부연안에서의 해수면변동

홍철훈 · 윤종환\*

부산수산대학교 해양산업개발연구소

\*큐우슈우대학 응용역학연구소

태풍통과시 동해의 일본북부연안에서의 수위변동을 조사하기 위해 1966~1986년간의 시간별수위자료분석 및 고분해능(5'×5')을 갖는 천해파모델상에서의 수치실험을 행하였다. 자료분석의 주결과는 1) 태풍통과시 Simonoseki(SS)와 Maizuru(MZ) 간에 약 4 m/s의 위상속도를 갖는 진행파가 존재하나, 2) Sasebo(SB)와 Hakata(HK) 간에는 파속이 매우 느리고(약 1.7 m/s), 3) HK에서는 SS에 비해 약 반나절 늦게 최대수위에 도달하는 점 등이었다. 실험결과는 관측결과와 좋은 대응을 보였다. 실험결과로 볼 때, 연안에 전파하는 진행파는 관측결과와 거의 같은 위상속도 약 4 m/s를 갖는 지형성파로서 확인된다. 태풍이 대한해협을 통과하기전에는 일본연안에 평행한 바람에 의해 생성된 남서방향의 연안젓트류에 의해 파의 전파가 영향을 받고, 태풍이 통과한 후에는 연안젓트류가 약해지면서 파가 전파하게 된다.